Korean J. Chem. Eng., 32(2), 350-353 (2015)
DOI: 10.1007/s11814-014-0280-3

pISSN: 0256-1115
eISSN: 1975-7220

Reactive radical cation transfer in the cages of icy clathrate hydrates

Dong-Yeun Koh, Hyery Kang, and Huen Lee†

Department of Chemical and Biomolecular Engineering, KAIST, 291, Daehak-ro, Yuseong-gu, Daejeon 305-701, Korea
(*Received 22 May 2014 • accepted 21 September 2014*)

Abstract−Clathrate hydrates are crystalline compounds consisting of hydrogen-bonded host water frameworks that eventually structure polyhedral cages. We suggest for the first time their potential as nano-reactors in which target reactions can occur. The energetics of one-dimensional CO radical cation ($CO^{\cdot+}$) transfers through the hexagonal faces of sI large cages are closely examined to verify the reaction concept in an icy confined space. The barrier energies for migrating a CO radical cation from the cage center to the edge of the hexagonal face are estimated to be 87 and 311 kJ/mol according to calculations with the B3LYP 6-311+G (d, p) basis set, significantly depending on the orientation of the radical. These results indicate that the barrier energy increases sharply when the CO radical cations are oriented parallel to the cage's hexagonal face. In the parallel migration mode, the hydrogen-bonded water networks are repulsed by electron clouds of $CO^{\cdot+}$ located on the same plane; thus, the repulsion forces induce a significant increase in the barrier energies. Further, we used separate basis sets of high and low levels processed by the ONIOM scheme for the effective calculation of the entire cage structure of the clathrate hydrates with guest molecules. The calculation run time was significantly shortened when the ONIOM scheme was adopted, while a difference in the barrier energy of approximately 5% was observed compared to the full-scale calculation with a high-level basis set.

Keywords: Clathrate Hydrate, CO_2, Structure I, Radical Cation, ONIOM

INTRODUCTION

"*Icy nano-reactor*" refers to the concept of using nano-sized hydrate cages as chemical reaction sites, emerging after the stable storage of radical species in a clathrate hydrate structure is confirmed. A sufficiently hydrophobic guest molecule has a tendency to occupy the empty site without significant host-guest interactions [1]. It thus acts as an isolated free molecule in the confined nano-sized empty space under mild temperature and pressure conditions. This type of stable existence of radical species in icy crystalline matrices may offer significant advantages in exploring clathrate hydrates as icy nano-reactors in which active reactions between guest radicals and ions can take place. More significantly, the novel designs and syntheses of ionic and radicalized icy clathrate hydrates are expected to open a new field in the areas of inclusion chemistry and ice-based science and technology.

The unique geometrical structure, the well-defined hydrogen bond network and the host-guest interactions in clathrate hydrates contribute to providing chemically (or physically) stable shelter for reactive hydrogen radicals and hydrocarbon radicals. It has been discovered that clathrate hydrate can be used as a medium for trapping radical species [2-8]. When hydrocarbon or binary clathrate hydrates are irradiated with g-rays, free radical species are formed. The lifetimes of these free radical species in the clathrate hydrate structures were confirmed by solid-state NMR spectroscopy and electron spin resonance (ESR). In a recent study, Yeon et al. [5] confirmed that the H_2+THF binary clathrate hydrate produces atomic hydrogen radicals through the g-ray irradiation of encaged H_2 molecules and THF molecules, noting that they were stably captured in small cages. Subsequently, using ionic guest species, Shin et al. [4] also confirmed atomic hydrogen generated from a water framework of γ-irradiated ionic clathrate hydrate ($Me_4NOH+16H_2O+N_2$) with the hydrogen radical stabilization effect of N_2 guest molecules in a dodecahedral cage. Koh et al. [8] proposed a highly efficient route for producing atomic hydrogen using semi-clathrate hydrates.

Furthermore, Ohgaki et al. [2] studied free hydrogen radical transfers in the propane hydrate system. They confirmed, using ESR in the 240-260 K temperature range, that when sII propane hydrates were irradiated with γ-rays, n-propyl and *i*-propyl radicals were formed. They showed that hydrogen radical transfers occur through the hexagonal faces of the large sII cages. Ohgaki et al. [2] concluded that an activation energy of 34±3 kJ mol^{-1} is needed to convert n-propyl radicals to *i*-propyl radicals in neighboring cages. Takeya et al. [3] explored the thermal stability of methyl radicals in methane hydrate using ESR in a temperature range of 210-260 K. They showed that when methyl radicals decay at higher temperatures, ethane molecules are generated by means of the dimerization process.

Atomic hydrogen radicals are much smaller than other hydrocarbon radicals and therefore diffuse relatively freely between cage networks, easily reacting as well with other radical species in the clathrate hydrate structure. Alavi et al. [9] characterized the energy barriers and migration rates of the H-radical in the clathrate hydrate medium. In their previous work, they [10] also showed that differences exist in the energy barriers during the migration of H_2 molecules through pentagonal faces (~105 kJ/mol) and hexagonal faces

†To whom correspondence should be addressed.
E-mail: hlee@kaist.ac.kr
‡This article is dedicated to Prof. Hwayong Kim on the occasion of his retirement from Seoul National Univerisity.

(~21 kJ/mol).

Studies of guest transfers between hydrate cages have thus far focused primarily on hydrogen molecules or hydrogen radicals. Hydrogen radicals and hydrogen molecules are smaller than other hydrocarbon species; therefore, these small species have the potential to travel between gas hydrate polyhedral cages. On the other hand, guest molecules larger than hydrogen molecules (hydrocarbons or carbon-based molecules) have rarely been studied in terms of their ability to transfer between hydrate cages. We focus here on cage transfers of the CO_2-derived radical species $CO^{\cdot+}$. CO_2 hydrate is one of the most common gas hydrates and is easily synthesized on a lab scale. Therefore, it is suitable for the study of nano-reactors with guest radical species. When CO_2 hydrate is irradiated with γ-rays at 77 K, various reactive chemical species are formed within the gas hydrate cages, such as $CO_2^{\cdot-}$, $CO^{\cdot+}$ and H· (hydrogen radicals deriving from the water frameworks). When the γ-irradiated CO_2 hydrates are thermally stimulated (up to 250 K), it is possible for a reaction to take place between these radical species inside the hydrate cages. For an icy water framework to act as a new reactive site, the enclosed space must first be created through a restructuring process of the host-guest network, after which the entrapped guest molecules are irradiated, forming a radical species. Next, radical species must travel among the cages to react freely and thus form the desired product. It is expected that this three-stage approach to developing an icy nano-reactor can be extended to a variety of organic host clathrates, which would significantly contribute to the technological development of radical reactions in icy matrices, gas storage using the inclusion phenomena of radical ions, and ice-based energy devices. The migration of hydrogen radicals between hydrate cages is a well-known phenomenon, but the migration of carbon-based substances has not been investigated thus far. Therefore, we focused on the possibility of using carbon monoxide radical cations as a reactive species by migration between cages. We employed MP2 and B3LYP calculations to determine the energy barrier for the transfer of $CO^{\cdot+}$ between hydrate cages through hexagonal/pentagonal faces.

COMPUTATIONAL DETAILS

We prepared a CO_2 sI hydrate structure with the lattice parameters and Cartesian coordinates of the sI hydrate. The charge distribution of guest molecules ($CO^{\cdot+}$) was defined using the QEq model [11]. The center of the cages was filled with $CO^{\cdot+}$ to simulate the radical transfer characteristics inside the icy lattice. To stabilize the cage structure, the positions of the hydrogen atoms were arranged to give the lowest dipole moment of the cage, i.e., about 0.75 Debye. The cage stability was checked by comparing the empty cage and the guest-filled cage. The empty cage had a base energy value of -1835 Hartree and the $CO^{\cdot+}$-filled cage had a base energy value of -1948 Hartree, providing evidence of the stabilization effect of the guest molecule.

The equilibrium structural parameters of the ground electronic state (S_0) for pure CO_2 hydrate were calculated using density-functional-theory (DFT) methods with the B3LYP functional basis set using the Gaussian 03 suite of programs. These parameters were used as a starting point for the $CO^{\cdot+}$ hydrate calculation [12]. Accordingly, we did calculations starting from 6-31G and going up to 6-311+G (d, p). The molecular energy and ONIOM calculations were also performed using the Gaussian 03 package.

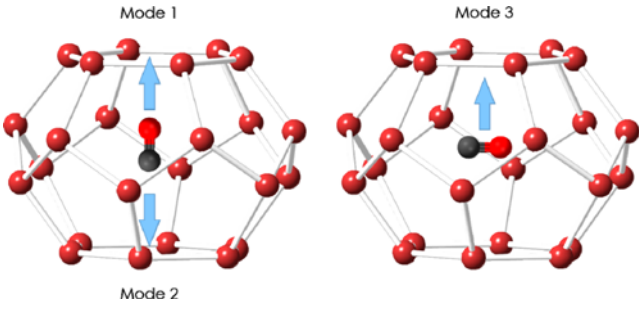

Fig. 1. Direction of the $CO^{\cdot+}$ perpendicular to the hexagonal face (left) and parallel to the hexagonal face (right). Barrier energies were calculated using three modes: (modes 1 and 2) perpendicular to the hexagonal face in the C and O direction, and (mode 3): parallel to the hexagonal face.

In the large cage of the structure I hydrate, $CO^{\cdot+}$ exists in an average position perpendicular or parallel to the hexagonal face of the cage. We separated the possible route of the $CO^{\cdot+}$ transfer between cages into three modes, as shown in Fig. 1: (mode 1) $CO^{\cdot+}$ perpendicular to the hexagonal face and in the C direction, (mode 2) $CO^{\cdot+}$ perpendicular to the hexagonal face and in the O direction, and (mode 3) $CO^{\cdot+}$ parallel to the hexagonal face. In mode 3, the direction of the $CO^{\cdot+}$ is perpendicular to the two opposing sides of the hexagonal face. The barrier energy may vary due to differences in the electron density of oxygen atoms and carbon atoms in $CO^{\cdot+}$. The calculations were conducted by varying the distance from the initial position (cage center) in steps of 0.3 Å.

RESULTS AND DISCUSSION

The barrier energies were calculated by varying the distance of the $CO^{\cdot+}$ from the sI large cage center. The results for mode 1 and mode 2 are shown in Fig. 2. When $CO^{\cdot+}$ started to move from the

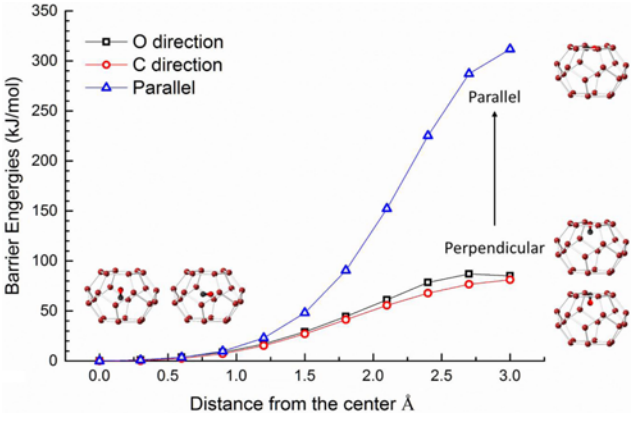

Fig. 2. Barrier energy differences in perpendicular mode (modes 1and 2) and in parallel mode (mode 3). The parallel mode shows a higher barrier energy level by fourfold compared to transfers in the perpendicular mode.

cage center to the hexagonal face of the cage (~3 Å away from the cage center), the barrier energy increased to 87 kJ/mol for mode 1 (C-direction) and to 81 kJ/mol for mode 2 (O-direction). $CO^{\cdot+}$ carries a charge which could influence the energy barrier to the inter-cage diffusion. From the calculation results of modes 1 and 2, we could conjecture that the charge distribution in $CO^{\cdot+}$ is slightly concentrated on the oxygen atom side. Oxygen atoms have higher electronegativity than carbon atoms and thus attract more electrons and create an asymmetric charge distribution. However, the difference in the potential energy barrier between two perpendicular modes is less than 7%. Therefore, we assumed that the atomic direction had no significant effect on the barrier energy during the radical transfer process. When the traveling direction of $CO^{\cdot+}$ changed to the parallel mode (mode 3), the barrier energies increased greatly to 311 kJ/mol. This barrier energy is nearly 3.5 times the barrier energy levels of modes 1 and 2. Fig. 2 shows the significant difference between the perpendicular modes and the parallel mode. The barrier energy calculation results suggest that the parallel traveling mode is severely restricted in the $CO^{\cdot+}$ case.

The barrier energies calculated in both cases of $CO^{\cdot+}$ transfer were higher than those of the hydrogen migration and hydrogen radical migration processes. Alavi et al. [10] calculated the barrier energy during H_2 migration in the sII large cage through the pentagonal face and the hexagonal face. In their calculation, the barrier energies increased to ~105 kJ/mol when H_2 molecules passed through the pentagonal face, while they remained at ~21 kJ/mol when the H_2 molecules passed through the hexagonal face. Furthermore, Alavi et al. [9] calculated the barrier energy during hydrogen radical migration in the sII large cage through the pentagonal face and the hexagonal face. For hydrogen radicals, the barrier energy decreased to ~61 kJ/mol when the hydrogen radicals passed through the pentagonal face and to ~17 kJ/mol when the hydrogen radicals passed through the hexagonal face. On the other hand, the CO radical cation is a free radical species with a positive charge that is much more reactive (much less stable) than other neutral species. Moreover, it has a charge distribution effect, as shown by calculation results of modes 1 and 2. Therefore, it is difficult make a direct comparison of the potential barrier energy during the inter-cage radical transfer process. However, the calculation results from neutral species are a good indicator for this if inter-cage diffusion can actually take place in the hydrate structure. Therefore, we used the values from neutral species calculations. The barrier energies of mode 1 and mode 2 were located between the barrier energy value of hydrogen radicals through the pentagonal face and these of H_2 through the pentagonal face. Comparing the hexagonal face results between H_2, hydrogen radicals and $CO^{\cdot+}$, the barrier energy in $CO^{\cdot+}$ was 4-17 times higher depending on the traveling mode.

To examine the origin of the differences in the barrier energies among the traveling modes, a highly simplified cage structure was adopted. We assumed that the increment in the barrier energy mostly stems from the interaction between the guest molecule and the hexagon. Therefore, we broke down the whole cage into a hexagon with $CO^{\cdot+}$ on the same plane and ran the same calculation again to observe the interaction between only the hexagonal face and $CO^{\cdot+}$. When the geometry optimization process was finished in the perpendicular mode, the hexagonal ring structure was soundly maintained during the calculation and was stabilized. However, in the parallel mode, the diameter of the hexagonal ring structure became wider during the geometry optimization process. The O-O distance between the farthest H_2O molecules in the hexagon is shown in Fig. 3. During the geometry optimization process, the value representing the O-O distance remained nearly the same in the perpendicular mode. However, ring widening was observed in the parallel mode. In the parallel mode, hydrogen-bonded water networks were repulsed by incoming $CO^{\cdot+}$ species, and the barrier energy thus increased. In the whole cage structure, the hexagonal face was tightly bound to other pentagonal faces and ring widening was restricted. As a result, the increase in the barrier energy while the $CO^{\cdot+}$ traveling process was ongoing was greater in the parallel mode (mode 3). In the whole-cage calculation results, the O-O distances in the hexagon did not significantly change during the geometry optimization process due to the limitation in the lattice positions. However, in single hexagon calculations, it was possible to observe the changes in the O-O distance, and we could determine that the increment in the barrier energy during the radical displacement process from the cage center was mostly due to the interaction between the hexagonal face and the $CO^{\cdot+}$. In conclusion, $CO^{\cdot+}$ travels through cages perpendicular to the hexagonal faces. The barrier energy calculation results using hexagon and $CO^{\cdot+}$ are shown in Fig. 3. When the calculation was performed using hexagon and $CO^{\cdot+}$, the total barrier energy value decreased to 80% of the value of the whole-cage calculation result. Therefore, we conjecture that the increment in the barrier energy during radical displacement from the cage center is mostly due to the interaction between the hexagonal face and the $CO^{\cdot+}$.

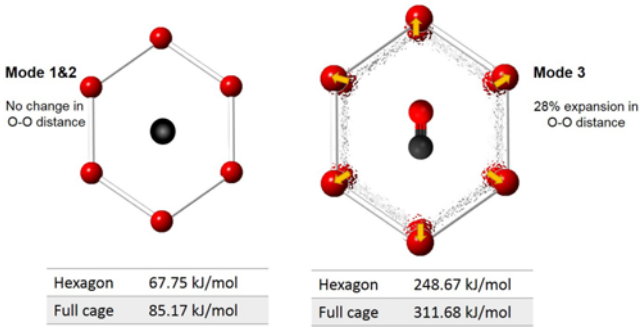

Fig. 3. Hexagonal face contribution in the barrier energy calculation. ~80% of the full cage calculation results are contributed by the hexagonal face.

Through the calculation using the single hexagon and $CO^{\cdot+}$, we observed that most of the increments in the barrier energies stemmed from the interaction between the guest molecule and the hexagon. This structural information allowed us to apply the ONIOM calculation method, which uses separate energy levels in the same structure. Therefore, we used the ONIOM scheme to calculate the barrier energy of the radical-filled cage structure and compared the results with those of the full-scale calculation (Fig. 4). In the ONIOM scheme, we separated the cage into two groups and applied different levels of calculation sets: (1) the hexagonal face and $CO^{\cdot+}$, B3LYP 6-311G+(d, p), and (2) the rest of the cage, HF 6-31G. When compared to the full-scale calculation results, the obtained barrier energy

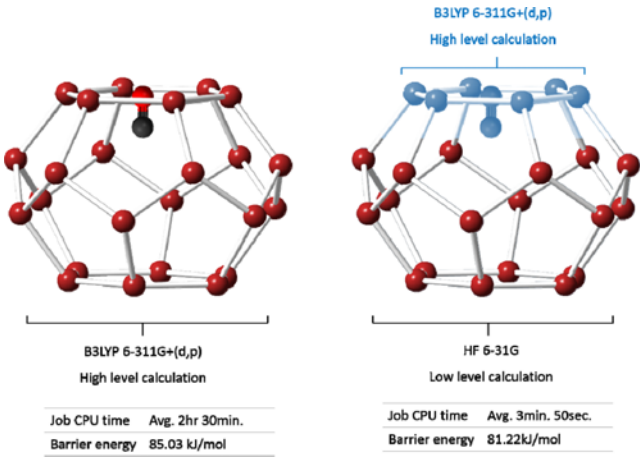

Fig. 4. Comparison of the full-scale calculation scheme (left) and the ONIOM scheme (right). In the ONIOM scheme, the hexagonal face and guest molecules were calculated using a high-level set (B3LYP 6-311 G+(d, p)) while other parts of the cages were calculated using a low-level set (HF 6-31G).

values were slightly lower. The difference in the barrier energies was ~4.5%. However, the ONIOM scheme provided significantly faster CPU run times (~2 hr 30 min in the full-scale calculation and 3-4 min in the ONIOM scheme calculation). When calculating the energy values related to clathrate hydrate compounds, these figures are very economical when applied to the ONIOM scheme.

CONCLUSION

We calculated how much barrier energy is present when $CO^{\cdot+}$ crosses the cages through the hexagonal face of structure I large cages. Depending on the traveling mode, the barrier energy changed significantly. For $CO^{\cdot+}$ in linearly shaped molecules, therefore, two traveling modes were used: perpendicular to the hexagonal face and parallel to the hexagonal face. Furthermore, atomic directions (C-direction and O-direction) were considered. When $CO^{\cdot+}$ crossed the cages, the perpendicular mode was preferred regardless of the atomic direction. The barrier energy increased sharply when $CO^{\cdot+}$ was parallel to the hexagonal face. In the parallel migration mode, hydrogen-bonded water networks were repulsed by incoming $CO^{\cdot+}$ species on the same plane. Therefore, the barrier energy increased. We also used separate basis sets, a high-level set and a low-level set, using the ONIOM scheme effectively to calculate the clathrate hydrate structure with guest molecules. The calculation run time was significantly shortened when the ONIOM scheme was adopted, while a difference of approximately 5% in the barrier energy was observed compared to the full-scale calculation with the high-level basis set.

ACKNOWLEDGEMENTS

This research was funded by the Ministry of Knowledge Economy through the "Recovery/Production of Natural Gas Hydrate using Swapping Technique" project [KIGAM-Gas Hydrate R&D Organization]. It was also supported by a grant from the National Research Foundation Korea (NRF) funded by the Korean government (MEST) (No. 2010-0029176) and by the WCU program (31-2008-000-10055-0), funded by the Ministry of Education and Science and Technology. This work is also funded by Brain Korea 21 plus project.

REFERENCES

1. E. D. Sloan and C. A. Koh, *Clathrate Hydrates of Natural Gases*, 3rd Ed., Boca Raton, CRC Press (2007).
2. K. Ohgaki, K. Nakatsuji, K. Takeya, A. Tani and T. Sugahara, *Phys. Chem. Chem. Phys.*, **10**(1), 80 (2008).
3. K. Takeya, K. Nango, T. Sugahara, K. Ohgaki and A. Tani, *J. Phys. Chem. B*, **109**, 21086 (2005).
4. K. Shin, M. Cha, H. Kim, Y. Jung, Y. S. Kang and H. Lee, *Chem. Commun. (Camb.)*, **47**(2), 674 (2011).
5. S.-H. Yeon, J. Seol, Y. Park, D.-Y. Koh, Y. S. Kang and H. Lee, *J. Am. Chem. Soc.*, **130**, 9208 (2008).
6. T. Sugahara, Y. Kobayashi, A. Tani, T. Inoue and K. Ohgaki, *J. Phys. Chem. A*, **116**(10), 2405 (2012).
7. N. Kobayashi, T. Minami, A. Tani, M. Nakagoshi, T. Sugahara, K. Takeya and K. Ohgaki, *Energies*, **5**(12), 1705 (2012).
8. D.-Y. Koh, H. Kang, J. Park, W. Shin and H. Lee, *J. Am. Chem. Soc.*, **134**(12), 5560 (2012).
9. S. Alavi and J. A. Ripmeester, *Chem. Phys. Lett.*, **479**(4-6), 234 (2009).
10. S. Alavi and J. A. Ripmeester, *Angew. Chem. Int. Ed.*, **46**(32), 6102 (2007).
11. A. K. Rappe and W. A. Goddard, *J. Phys. Chem.*, **95**(8), 3358 (1991).
12. M. J. Frisch, G. W. Trucks, H. B. Schlegel, G. E. Scuseria, M. A. Robb, J. R. Cheeseman, J. A. Montgomery, Jr., T. Vreven, K. N. Kudin, J. C. Burant, J. M. Millam, S. S. Iyengar, J. Tomasi, V. Barone, B. Mennucci, M. Cossi, G. Scalmani, N. Rega, G. A. Petersson, H. Nakatsuji, M. Hada, M. Ehara, K. Toyota, R. Fukuda, J. Hasegawa, M. Ishida, T. Nakajima, Y. Honda, O. Kitao, H. Nakai, M. Klene, X. Li, J. E. Knox, H. P. Hratchian, J. B. Cross, V. Bakken, C. Adamo, J. Jaramillo, R. Gomperts, R. E. Stratmann, O. Yazyev, A. J. Austin, R. Cammi, C. Pomelli, J. W. Ochterski, P. Y. Ayala, K. Morokuma, G. A. Voth, P. Salvador, J. J. Dannenberg, V. G. Zakrzewski, S. Dapprich, A. D. Daniels, M. C. Strain, O. Farkas, D. K. Malick, A. D. Rabuck, K. Raghavachari, J. B. Foresman, J. V. Ortiz, Q. Cui, A. G. Baboul, S. Clifford, J. Cioslowski, B. B. Stefanov, G. Liu, A. Liashenko, P. Piskorz, I. Komaromi, R. L. Martin, D. J. Fox, T. Keith, M. A. Al-Laham, C. Y. Peng, A. Nanayakkara, M. Challacombe, P. M. W. Gill, B. Johnson, W. Chen, M. W. Wong, C. Gonzalez and J. A. Pople, *Gaussian 03* (2003).